


Cite this: *RSC Adv.*, 2022, 12, 7680

# Sensitive and specific capture of polystyrene and polypropylene microplastics using engineered peptide biosensors†

Hyunjeong Woo,<sup>a</sup> Seung Hyun Kang,<sup>e</sup> Yejin Kwon,<sup>a</sup> Yonghyun Choi,<sup>a</sup> Jiwon Kim,<sup>a</sup> Don-Hyung Ha,<sup>id</sup><sup>a</sup> Masayoshi Tanaka,<sup>b</sup> Mina Okochi,<sup>id</sup><sup>b</sup> Jin Su Kim,<sup>cd</sup> Han Koo Kim<sup>\*e</sup> and Jonghoon Choi<sup>id</sup><sup>\*a</sup>

Owing to increased environmental pollution, active research regarding microplastics circulating in the ocean has attracted significant interest in recent times. Microplastics accumulate in the bodies of living organisms and adversely affect them. In this study, a new method for the rapid detection of microplastics using peptides was proposed. Among the various types of plastics distributed in the ocean, polystyrene and polypropylene were selected. The binding affinity of the hydrophobic peptides suitable for each type of plastic was evaluated. The binding affinities of peptides were confirmed in unoxidized plastics and plasma-oxidized plastics in deionised or 3.5% saline water. Also, the detection of microplastics in small animals' intestine extracts were possible with the reported peptide biosensors. We expect plastic-binding peptides to be used in sensors to increase the detection efficiency of microplastics and potentially help separate microplastics from seawater.

Received 29th November 2021

Accepted 19th February 2022

DOI: 10.1039/d1ra08701k

rsc.li/rsc-advances

## Introduction

Plastics have diverse applications in various industries because they are easy to use, easy to synthesise, lightweight, and semi-permanent. In general, the use of plastics is rapidly increasing worldwide due to an increased demand.<sup>1–4</sup> Although plastic remains a difficult resource for recycling, the recent COVID-19 outbreak has led to an even greater use of plastics in the form of disposable packaging for containers and tableware. A large amount of such plastic material ends up in the garbage and eventually gets buried in landfills or flows into the sea. As they circulate in the sea, plastics with low specific gravity fragments become microplastics. These microplastics follow ocean currents and affect the environment.<sup>5,6</sup>

Microplastics are 5 mm or smaller in size.<sup>7</sup> Depending on the process of manufacturing, they can be divided into primary and secondary microplastics. Primary microplastics are deliberately

manufactured in small sizes, for example, the plastics present in toothpaste, abrasives, and cosmetics. In contrast, secondary microplastics are those that are transformed into microscopic sizes because of the influence of physical forces (*e.g.*, rain, wind, or waves), chemical forces (*e.g.*, ultraviolet radiation from sunlight, temperature, or corrosion), or biodegradation (*e.g.*, microorganisms).<sup>8–11</sup> Microplastics float in rivers and seas and are ingested along with food by various living organisms.

Various types of plastics are distributed in the sea, and the type and amount of distributed plastic are detected in proportion to the amount of plastic used worldwide. PP (polypropylene), PE (polyethylene), and PS (polystyrene) are the most used plastics; therefore, they account for the largest proportion.<sup>9–14</sup> In the conventional microplastic detection method, samples are first collected from oceans, rivers, and land and then pre-treated to remove organic and inorganic substances. Subsequently, optical microscopy, Fourier-transform infrared (FTIR) spectroscopy, Raman spectroscopy, and scanning electron microscopy (SEM) are used to detect and classify microplastics by size, type, and shape.<sup>15–17</sup> For pre-treatment, H<sub>2</sub>O<sub>2</sub> or Fenton's reagent is generally used. Although microplastics can be separated based on density differences, using NaCl or NaI, the effectiveness of such separation procedures is limited and depends on the type of microplastic.<sup>18</sup> However, this pre-treatment is time-consuming and labour-intensive.<sup>19–21</sup> In the case of microscopic techniques, such as SEM, the accuracy of distinguishing among the various types of microplastics is poor, and the process is time consuming. In contrast, in the case of FTIR or Raman spectroscopy, a large amount of data can be

<sup>a</sup>School of Integrative Engineering, Chung-Ang University, Seoul 06974, Republic of Korea. E-mail: nanomed@cau.ac.kr

<sup>b</sup>Department of Chemical Science and Engineering, Tokyo Institute of Technology, 2-12-1-S1-24, O-okayama, Meguro-ku, Tokyo 152-8552, Japan

<sup>c</sup>Division of RI Application, Korea Institute Radiological and Medical Sciences, Seoul 01812, Republic of Korea

<sup>d</sup>Radiological and Medico-Oncological Sciences, University of Science and Technology (UST), Seoul 01812, Republic of Korea

<sup>e</sup>Department of Plastic and Reconstructive Surgery, Chung-Ang University Hospital, Seoul, 06973, Republic of Korea

† Electronic supplementary information (ESI) available. See DOI: 10.1039/d1ra08701k



collected over a short period of time by using the available libraries for specific chemicals, molecules, and bonds. However, these methods have technical limitations. For instance, these libraries contain insufficient data to determine the specific surface chemical structures of plastics. In addition, there is a high probability of misrecognition by FTIR or Raman spectroscopy due to the various types, shapes, and sizes of microplastics as well as the changes in the environmental surface conditions. The smaller the size of the microplastic, the closer it is to the detection limit of the device; this makes accurate analysis challenging and time-consuming.<sup>17,22,23</sup> Dyeing methods have also been developed for the detection of plastics. Among them, Nile red staining is the most representative method.<sup>24</sup> Nile red staining produces different spectra depending on the environment of the sample, and the dye binds to the polymer surface through van der Waals interactions. After dyeing with Nile red, the wavelength range in which the actual fluorescence is observed varies depending on the type of the plastic. Although dyeing works well for hydrophobic materials such as PE and PP, it is difficult to dye polar plastics, such as PVC and PET, with Nile red.<sup>25</sup> Additionally, since Nile red is poorly soluble in water, an organic solvent must be used, which lengthens the process because the pre-treatment and separation of plastics are required. Moreover, coloured plastics containing dyes cannot be stably dyed because the dye affects the affinity of the plastic to Nile red.<sup>26</sup> Furthermore, Nile red is used to stain various biological materials besides microplastics; thus, it can yield false-positive results. Antibodies are sometimes used to achieve high sensitivity and selectivity during the detection of plastics. However, antibodies are susceptible to environmental factors such as temperature changes and are thus not suitable for long-term storage or field applications.<sup>27,28</sup> In addition, the production process is complicated, which makes the use of antibodies difficult owing to the high price involved.<sup>29</sup>

Studies on peptides that bind to PS and PP have been conducted since the late 1990s. Peptides incur a lower production cost than antibodies. Moreover, a large-capacity, high-efficiency screening can be achieved while using phage display. In addition, the stability, selectivity, and sensitivity of peptides towards microplastics can easily be controlled by properly designing the amino acid combination.<sup>30–33</sup> Since the both two plastics selected for this study (PS and PP) have a hydrophobic chemical structure, we attempted to detect microplastics through peptides using the ability of peptides and plastics to form hydrophobic bonds. Peptides that bind to PS and PP (PSBPs and PPBPs) were selected for their hydrophobic properties (Fig. 1). In addition, considering that microplastics exposed to the environment will exist in an oxidized state due to exposure to factors such as UV radiation and ocean waves,<sup>6,10</sup> the surface of the microplastics was intentionally oxidized using O<sub>2</sub> plasma.<sup>34,35</sup> The peptide affinities of normal and oxidized microplastics were then evaluated. As peptides may be used in the future to detect microplastics that are distributed in aquatic environments, such as oceans and rivers, peptide affinities were evaluated in deionised water and a 3.5% NaCl solution to mimic conditions

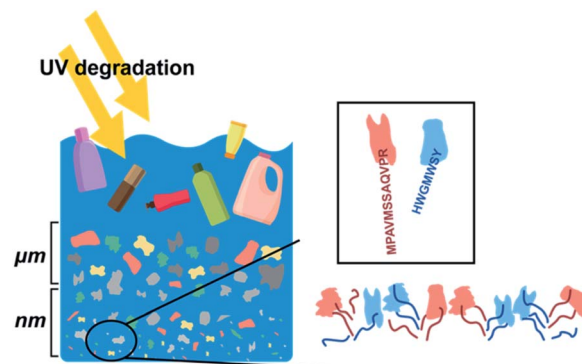


Fig. 1 Schematic of the fragmentation of plastics in seawater. Peptides that have amino acid sequences that bind to specific plastics are also shown.

similar to those in the sea. Based on the results of this study, we expect that microplastic PS and PP can be detected more efficiently and conveniently using peptides than with the existing technologies.

## Experimental

### Materials

PS (average  $M_w$ : 35 000) and PP (average  $M_w$ : ~12 000) were purchased from Sigma-Aldrich (St. Louis, MO, USA). Glass vials (part number: 5182-0546) were purchased from Agilent Technologies (SC, CA, USA). PS microspheres (part number: PSMS-1.07, diameter 9.5–11.5  $\mu$ m) and PE microspheres (UVPMS-BG-1.00) were purchased from Cospheric (SB, California, USA). Hydrochloric acid (Cat. H1758) and Tween-80 (Cat no. 28329) were purchased from Sigma-Aldrich. Methyl alcohol and NaCl were purchased from Daejung (Siheung-si, Gyeonggi-do, Korea). The 96-well cell culture plates were purchased from SPL Life Sciences (Pocheon-si, Gyeonggi-do, Korea). The Q500 sonicator was purchased from Q-Sonica (Newtown, CT, USA). The plastic-binding peptides FITC-Ahx-HWGMWSY (PSBP), FITC-Ahx-MPAVMSSAQVPR (PPBP), and FITC-Ahx-LPPWKHKTSOVA (PEBP) were acquired from Anygen (Buk-gu, Gwangju, Korea). The feeding needles (Cat no. JD-S-124) were purchased from JEUNG DO B&P (Nowon-gu, Seoul, Korea). Water, which was used to combine the peptides with the plastics, was purified using a Millipore Milli-Q system (18.2 M $\Omega$  cm resistance).

### Preparation of the microplastics

PS and PP were pulverised into small pieces using a blender (UNIX, UNB-A9100, Seoul, Korea). The pulverised plastics were separated based on size using a testing sieve (Chunggye sieve; Gunpo-si, Gyeonggi-do, Korea) with mesh sizes of 106, 75, 53, and 38  $\mu$ m. To verify the accuracy of the separation based on size, samples were examined through a microscope after blending and then analysed by drawing a size distribution diagram through ImageJ.



## Selection of peptides

Since PS and PP are both hydrophobic plastics, hydrophobic peptides were selected with the intention of plastic bonding of the peptides through hydrophobic interactions. The hydrophobicity of each peptide was calculated using the following formula:

$$\text{Hydrophobicity of peptides (\%)} = \frac{\text{number of amino acid with hydrophobic chain}}{\text{number of total amino acid}} \times 100$$

## Oxidation of plastics

PP and PS beads were used for surface oxidation. The plastic surfaces were oxidized in the form of beads. After lowering the base pressure to  $5 \times 10^{-2}$  Torr, the samples were treated with  $\text{O}_2$  gas at 50 sccm for 3 min. Subsequently, plasma oxidation was performed using 70 W 50 kHz plasma for 3 min. The oxidized plastic was then pulverised using the method described above to obtain the oxidized microplastics.

## FTIR spectrometry

The FTIR spectra of the oxidized and unoxidized plastic samples were obtained using an Alpha II spectrometer (Bruker, Billerica, MA, USA) to confirm their surface chemical properties. The measurement baseline was set to a blank surface that did not have a sample placed at the measurement location. The samples used consisted of native (non-oxidized) PS, native PP, oxidized PS, and oxidized PP in bead form.

## Evaluation of the efficiency of peptides bound to the microplastics

Since the microplastics chosen for detection were hydrophobic, a hydrophobic plastic-binding peptide was selected. Among the PSBPs mentioned in the literature, an appropriate PSBP was determined using the PSBinder software.<sup>36</sup> For example, HWGMWSY, an unexpected polystyrene-binding peptide, was chosen from the random phage display libraries.<sup>37</sup> PPBP was used in the experiment by selecting the most hydrophobic of the seven sequences in the US patent.<sup>38</sup> PSBP and PPBP solutions with concentrations of 10, 5, 1, and  $0.5 \mu\text{g mL}^{-1}$  were prepared by dilution with DI water and a 3.5% NaCl solution. Approximately 2 mg of microplastics (size ( $\bar{x}$ ) >  $106 \mu\text{m}$ ) was added to each glass vial, along with 1 mL of the peptide solution. The vial was fixed in a multi-mixer (SLRM-3; SeouLin Bioscience, Seongnam, Gyeonggido) and rotated in the F1 mode at 35 rpm for 3 h to induce binding of the plastic to the peptide. After 3 h, the solution was transferred to an e-tube to measure the concentrations of unbound free peptides. An additional 0.7 mL of washing solution (containing methanol : DI water in a 7 : 3 ratio) was used to collect all the microplastics remaining in the glass vials. The solutions were washed thrice for 5 min each at 13 000g using centrifugation. The concentrations of the free peptides in the three separated supernatants were determined using fluorescence measurements that were obtained at

excitation and emission wavelengths of 485 nm and 520 nm, respectively, using a plate reader (Synergy H1; BioTek, Winooski, VT, USA). A standard curve was drawn for each plastic-binding peptide (PBP) solution, and the concentration of the bound peptide was calculated using linear regression.

To determine the peptide-binding degree of the oxidized and unoxidized microplastics, PSBP and PPBP solutions with  $10 \mu\text{g mL}^{-1}$  concentration were subjected to the same experimental procedure as described above.

## Animal care and PS feeding

All animal experiments were performed according to the institutional guidelines of the Korea Institute of Radiology and Medical Sciences (KIRAMS). All protocols were approved by the institutional animal care and use committee (IACUC number: KIRAMS 2020-0015). C57BL/6J mice (Shizuoka Laboratory Center, Japan) were 5–6 weeks old at the beginning of the experiments. The animals were weighed, caged, housed, and maintained for 24 h under a 12 h light/dark cycle.

For PS and PE feeding, PS microspheres (Cospheric, USA) were reconstituted in Tween-80 (Sigma, USA) to prepare a 10% weight/volume stock solution. The stock solution was homogenised using a sonicator (Q-Sonica, USA). After dilution, 100 ppm/100  $\mu\text{L}$  of PS was orally administered to mice daily for a total of four weeks. A sterile single-use animal-feeding needle was used.

## Organ lysis

After feeding with PS for 4 weeks, the mice were euthanised using  $\text{CO}_2$ . Subsequently, the small intestines of the mice were extracted. The extracted organs were lysed overnight using hydrochloric acid (Sigma, USA, 5 mL), at room temperature, in a glass vial. The lysed tissue was sonicated for 5 min.

## Determination of the presence or absence of microplastics in the lysed tissue

The lysed tissue was neutralised with NaOH and filtered through a syringe filter with a  $0.2 \mu\text{m}$  pore size. The microplastic particles present in the filtrate were detected from mouse tissues. These mice were orally administered green fluorescence-labelled PE particles of approximately  $20 \mu\text{m}$  size.

## Confirmation of bonding between peptide and PS particles in tissue lysate

To confirm the binding of the plastic and peptide, mice were fed non-fluorescent PS particles. After following the aforementioned process used for PE particles, the filtered lysate was freeze-dried to obtain a powder. A binding confirmation experiment using PSBP was performed with the tissue particles thus obtained. The lysed powder ( $100 \text{ mg mL}^{-1}$ ) and PSBP ( $10 \mu\text{g mL}^{-1}$ ) were dissolved in 1 mL of DI water and rotated using a multi-mixer for 3 h. Thereafter, the binding of PSBP to PS particles was examined using a fluorescence microscope.



## Results and discussion

PS and PP, which are the most commonly distributed types of plastics found in the ocean, were selected to evaluate the detection capability of the peptides. To obtain the microplastic samples, PS and PP plastic beads were crushed and separated by size using a sieve. Microplastics distributed in nature are reduced by UV radiation and exist in various sizes. Microplastic samples were prepared for experimentation by mimicking the size distribution in nature. The crushed samples were separated into different size ranges based on the size interval of the sieve eye. The samples in the smallest size range ( $53\ \mu\text{m} > x > 38\ \mu\text{m}$  or less) were difficult to separate from the sieve because of static electricity. Therefore, the yield was very low, and samples of this size range were not used in the experiments.

Fig. 2 shows the frequency distribution of the sizes measured for the crushed PS and PP samples. Both the PS and PP particles exhibited an average size of  $100\ \mu\text{m}$  for the samples separated with the  $106\ \mu\text{m} > x > 75\ \mu\text{m}$  sieve. The average sizes were confirmed to be  $60\ \mu\text{m}$  and  $30\ \mu\text{m}$  for the samples obtained by separation with the  $75\ \mu\text{m} > x > 53\ \mu\text{m}$  and  $53\ \mu\text{m} > x > 38\ \mu\text{m}$  sieves, respectively. Fine plastics smaller than  $38\ \mu\text{m}$  in size could not be properly separated because of static electricity. Thus, plastics of various sizes, particularly those with a minimum size of  $10\ \mu\text{m}$ , can be obtained through mixer grinding.

As plastics that exist in the environment are mostly oxidized due to exposure to the elements, oxidized microplastics were synthesised through surface oxidation *via*  $\text{O}_2$  plasma and then pulverised. The differences between the chemical structures of the oxidized and unoxidized plastic samples were determined using FTIR spectral results (Fig. 3). In the FTIR spectra of the PS and PP samples with and without oxidation, excitation peaks were observed at  $1650\ \text{cm}^{-1}$  and  $3100\text{--}3500\ \text{cm}^{-1}$ , respectively. Based on the available literature, the peak at  $1700\ \text{cm}^{-1}$  was attributed to the carbonyl group ( $\text{C}=\text{O}$ ), while the band at  $3100\text{--}3500\ \text{cm}^{-1}$  was attributed to the hydroxyl group ( $\text{C}-\text{O}$ ). When the samples were oxidized, the intensities of the peaks

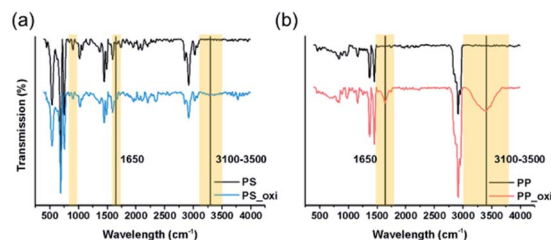


Fig. 3 FTIR spectra obtained after polystyrene and polypropylene surface oxidation using plasma. (a) Polystyrene and (b) polypropylene.

increased.<sup>39–42</sup> Moreover, the FTIR band in the  $1700\text{--}1800\ \text{cm}^{-1}$  range was attributed to the carbonyl group; this band indicated surface oxidation. However, in the case of oxidized microplastics, this band shifted to approximately  $1650\ \text{cm}^{-1}$ . Therefore, in our study, the band at  $1650\ \text{cm}^{-1}$  was attributed to oxidation.<sup>39,40</sup>

In addition, FTIR results of the microplastics obtained from nature were compared with those of the plasma-oxidized samples obtained in our study. The FTIR results of the plasma-oxidized samples were found to be similar to those of the microplastics obtained in nature.<sup>13,43</sup> These data confirmed the surface oxidation of PS and PP.

Different types of plastic-binding peptides (PSBP, PPBP, and PEBP) were used depending on the type of plastic, and the binding strengths between the peptide and microplastic were evaluated. To determine the binding of the plastic more intuitively to the peptide, FITC (fluorescein isothiocyanate) was attached to the end of each peptide. First, to confirm the affinity of the peptide to the microplastics, the optimal peptide concentration was determined. Based on previous research, the highest ( $10\ \mu\text{g mL}^{-1}$ ) and lowest ( $0.5\ \mu\text{g mL}^{-1}$ ) possible concentrations were determined. Since the ultimate intention was to use peptides for the detection of microplastics distributed in the ocean, the binding reaction was performed in a 3.5% NaCl solution to simulate seawater.<sup>44–48</sup>

The existing literature was investigated to select a peptide that binds to the plastic. Regarding PSBP, many studies have immobilised the antibody on the plate using assay techniques such as the ELISA method.<sup>45,49</sup> Since the PS plate used for ELISA undergoes a hydrophilic surface treatment, PSBP is usually selected for optimal binding to hydrophilic PS.<sup>50</sup> As hydrophobic PS was used in this study, hydrophobic peptides were selected. Studies on PPBP and PEBP have been conducted to increase their affinity towards plastic binding by modifying some of the amino acids of the protein rather than a single peptide sequence. To select the peptide sequence to be used in this experiment, a search of patents was also conducted.<sup>51,52</sup> In addition, to ensure the specificity of the peptide to the plastic, the binding of PPBP and PEBP to PS was verified in advance through the PSBP prediction software, and the peptides that did not bind to PS were not considered. Based on the results, the final PSBP, PPBP, and PEBP sequences were selected by considering the number of papers in which the sequences were cited and the hydrophobicity of the peptides (Tables 1–3).

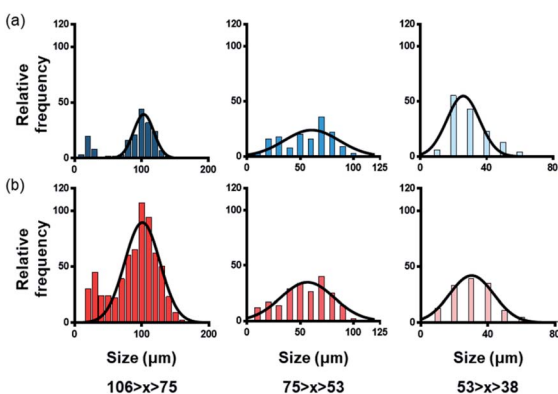


Fig. 2 Size distribution of micro-polystyrene and micro-polypropylene obtained after grinding and separation with various sieve eyes. (a) Polystyrene and (b) polypropylene.



Table 1 Polystyrene-binding peptides reported in papers and patents

Sequence	Length	Hydrophobicity (%)
RAFIASRRIRKP <sup>53</sup>	12	33
RAFIASRRIRRP <sup>44</sup>	12	33
RIIRIRRR <sup>44</sup>	9	44
HWGMWSY <sup>37</sup>	7	57
KLWWMIRRW <sup>54</sup>	9	67
LKKLLKLLKLLKL <sup>55</sup>	14	57
TLHPAAD <sup>33</sup>	7	43
KGLRGWREMISL <sup>48</sup>	12	42
TSTASPTMQSKIR <sup>38</sup>	13	15
KRNHWQRMHLSA <sup>38</sup>	12	23
SHATPPQGLGPQ <sup>38</sup>	12	17
PRAGSYRRAFRA	23	39
QLKRANFPTLR <sup>56</sup>		

Fig. 4 shows the binding affinities of the peptides to microplastics, which were obtained at various peptide concentrations in DI water and a 3.5% NaCl solution. In previous studies, peptide concentrations in the range of 1–10  $\mu\text{g mL}^{-1}$  were considered. Using this as the basis, we conducted experiments at peptide concentrations of 10  $\mu\text{g mL}^{-1}$ , 5  $\mu\text{g mL}^{-1}$ , 1  $\mu\text{g mL}^{-1}$ , and 0.5  $\mu\text{g mL}^{-1}$ .<sup>44–48</sup> The binding efficiency was confirmed by measuring the fluorescence of FITC, which was obtained after binding to the plastic. FITC was attached to the end of the peptide. In DI water, approximately 50% of PS and PP were bound to the peptide at a concentration of 10  $\mu\text{g mL}^{-1}$ . In contrast, in 3.5% NaCl solution, at a peptide concentration of 10  $\mu\text{g mL}^{-1}$ , approximately 20% of PS and 50% of PP were combined. As shown in

Table 2 Polypropylene-binding peptides reported in patents<sup>38</sup>

Sequence	Length	Hydrophobicity (%)
TSDIKSRSPHHR	12	8.3
HTONMRMYEPWF	21	41.67
LPPGSLA	7	42.86
MPAVMSSAOVPR	12	50
NOSFLPLDFPFR	12	41.67
SILSTMSPHGAT	12	25
SMKYSHSTAPAL	12	41.67

Table 3 Polyethylene-binding peptides reported in patents<sup>38</sup>

Sequence	Length	Hydrophobicity (%)
HNKSSPLTAALP	12	8.3
LPPWKHKTSQWA	21	41.67
LPWWLRDSYLLP	7	42.86
WPWWKHPLPLPW	12	50
HHKOWHNHPHHA	12	41.67
HIFSSWHOMWHR	12	25
WPAWKTHPILRM	12	41.67

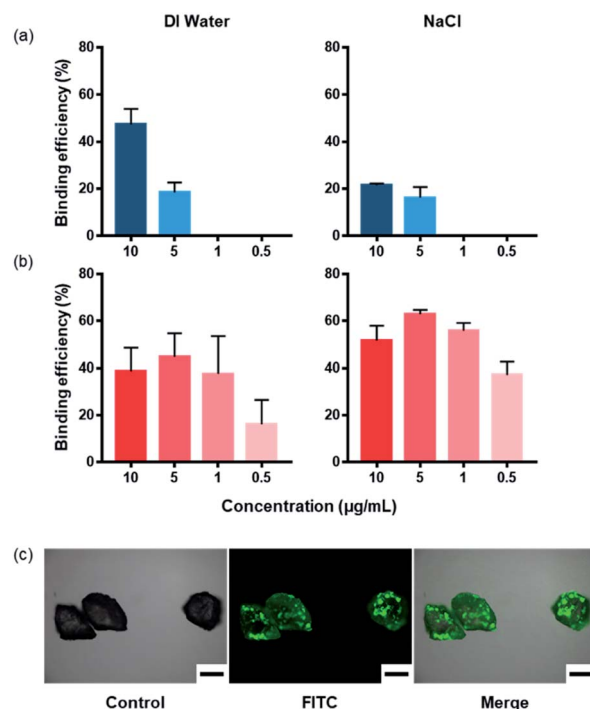


Fig. 4 Binding affinity of peptides with various concentrations of microplastics. Solutions with peptide concentrations of 10  $\mu\text{g mL}^{-1}$ , 5  $\mu\text{g mL}^{-1}$ , 1  $\mu\text{g mL}^{-1}$ , and 0.5  $\mu\text{g mL}^{-1}$  were prepared and allowed to react with the target plastic. The optimal peptide concentration in DI Water and 3.5% NaCl solution was determined to be 10  $\mu\text{g mL}^{-1}$ . (a) Polystyrene and (b) polypropylene. (c) Photographs of peptides bound to polypropylene (PPBP, 10  $\mu\text{g mL}^{-1}$ , DI water). Scale bar: 100  $\mu\text{m}$ .

Fig. 4(a), in the case of PS, fluorescence could not be measured at peptide concentrations of 1  $\mu\text{g mL}^{-1}$  and 0.5  $\mu\text{g mL}^{-1}$  in both the DI water and 3.5% NaCl solution because the binding of the peptide was lower than the detection limit of fluorescence. Furthermore, in the case of PP, there were no significant differences in the fluorescence values between the DI water and 3.5% NaCl solution at a peptide concentration of 10  $\mu\text{g mL}^{-1}$ . However, in the case of PS, the difference in binding efficiency between the two solutions was approximately 30%, and it was concluded that the optimal concentration of the peptide was 10  $\mu\text{g mL}^{-1}$ . Subsequent experiments were performed at these concentrations. Based on the fluorescence microscopic results, the microplastics and peptides were

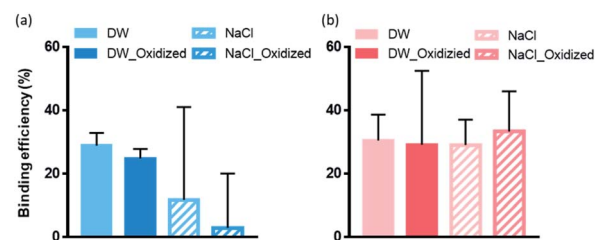


Fig. 5 Peptide-binding efficiency of the oxidized plastics in DI water and 3.5% NaCl solution. "Oxidized" refers to the plastic samples with plasma-oxidized surfaces. (a) Polystyrene and (b) polypropylene.



confirmed to be bound at a peptide concentration of  $10\ \mu\text{g mL}^{-1}$  (Fig. 4(c)).

The binding efficiencies between the plastic and peptides were evaluated in DI water and 3.5% NaCl solution using microplastic samples with and without surface oxidation treatments (Fig. 5, ESI Fig. S1 and S2†). PS and PP exhibited similar binding efficiencies in DI water and 3.5% NaCl solution, regardless of oxidation treatment. However, in the case of PS, the binding efficiency of the peptide was lower in the 3.5% NaCl solution than in DI water. According to literature, NaCl interferes with the binding of the amine group in the basic amino acid arginine when it binds to the surface of the PS plate.<sup>44</sup> Although the peptides selected in this study were hydrophobic, the presence of the basic amino acids, arginine and histidine, in the sequence was expected to lower the binding efficiency in the presence of NaCl. In addition, the  $\pi$ - $\pi$  interactions affect the binding of PS and the peptides. This is because the  $\pi$ - $\pi$  interactions are affected by the hydrophobic interactions as well as the Hofmeister series. As the ion concentration increases, protein solubility decreases. Therefore, the solubility of the peptides in the NaCl solution decreases, which is expected to affect the binding of the peptide to the plastic.<sup>57–59</sup> Furthermore, PSBP tends to have a lower overall binding efficiency with the target microplastics than PPBP, which is believed to be due to the aforementioned characteristics of PSBP. Furthermore, PSBP is more hydrophobic than PPBP, which further inhibits its affinity to the plastic due to peptide aggregation.

To evaluate binding selectivity of the peptides to plastic, the binding efficiency of PEBP with regard to PP was experimentally investigated in DI water and 3.5% NaCl solution. In DI water, approximately 50% of the peptide was combined, whereas in the 3.5% NaCl solution, approximately 10% of the peptide was combined at a concentration of  $10\ \mu\text{g mL}^{-1}$  (supporting Fig. 3(a)). Next, at the optimal peptide concentration of  $10\ \mu\text{g mL}^{-1}$ , we investigated the tendency of PEBP to bind to the oxidized PP. In DI water, approximately 40% of the PEBP bound to PP, regardless of surface oxidation, and in 3.5% NaCl solution, the binding efficiency decreased to approximately 10% (supporting Fig. 3(b)). This is attributed to the presence of more basic amino acid groups in PEBP than in PPBP. As a result, there is a greater impact from NaCl in the case of PEBP.<sup>44</sup> The effect of peptide-binding efficiency on the degree of fluorescence of the peptide located on the plastic surface was also visually studied through a fluorescence microscope (supporting Fig. 2 and 3(c)). The binding efficiencies of PEBP and PPBP to PP in DI water were found to be similar, whereas in the 3.5% NaCl solution, PPBP exhibited a higher extent of binding to PP than PEBP. Therefore, we propose that PPBP demonstrates better selectivity towards PP than PEBP in an environment with high interference to binding.

An experiment was designed to determine whether the peptides we selected bound well to the microplastics that exist in natural environments. Microplastics that exist in nature are either distributed in a state exposed to the environment or accumulated in the bodies of living organisms *via* ingestion with food.<sup>16,60</sup> Microplastics ingested in this way go through a digestive process; their size decreases, and their surface is

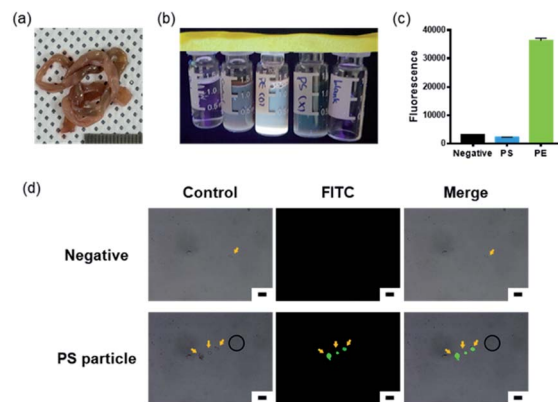


Fig. 6 Confirmation of the binding of peptides to plastics (PS) accumulated in the body of mice. The binding was confirmed by dissolving the small intestine tissues of C57BL/6J mice fed with or without microplastics and binding them with peptides. (a) Small intestine tissue. Scale bar: 1 mm. (b) Fluorescence confirmation at 365 nm after  $0.2\ \mu\text{m}$  filtration. From left, DI water, negative control (lysed tissue of the small intestines of the plastic-non-fed mice), lysed tissue from the PE particle-fed mice, lysed tissue from PS-fed mice and blank (empty glass vial). (c) Fluorescence measurement of lysed tissue after  $0.2\ \mu\text{m}$  filtration. (d) Fluorescence microscopic image after binding the lysed tissue with peptide. Scale bar:  $50\ \mu\text{m}$ .

oxidized by enzymes and digestive juices in the body.<sup>61</sup> To mimic this, microplastic particles were orally administered. To confirm the bonding process between the plastic and the peptide, the small intestines, the organ where the digestion process takes place, were selected as the test subject (Fig. 6(a)).

The small intestines extracted from mice orally administered with PS particles were dissolved in HCl and then neutralised to pH 7 using NaOH. The samples were then filtered through a syringe filter to remove foreign substances, such as undissolved tissue and dust. To assess whether microplastic particles remained in the lysed filtrate after filtration, tissues of mice orally administered with fluorescence-labelled PE particles were used. When the samples were irradiated with UV (365 nm wavelength), fluorescence was particularly observed in samples with PE particles (Fig. 6(b)). In addition, when the fluorescence value for each sample was assessed, the same result was obtained (Fig. 6(c)). This indicates that filtration did not affect the microplastic particles. However, auto-fluorescence was also observed in the small intestine tissue of the negative control group, mice that were not fed with plastic. Subsequent experiments were carried out after considering this observation. As shown in Fig. 6(d), almost no peptide was bound to the particles present in the negative control group. In the PS particle test group, the peptide bound to the PS microplastic particles showed green fluorescence. The particles were smaller than approximately  $20\ \mu\text{m}$ ; hence, the PS particles administered as food became slightly smaller during digestion. This indicates that PSBP binds to the PS particle surface even during the digestion and oxidation processes. Based on these observations, we confirmed that PSBP, which was selected in this study, could also bind to PS particles that exist in nature.

## Conclusions

Based on the results of this study, we confirmed that the selected peptides, PSBP and PPBP, could bind to unoxidized and oxidized microplastics. As both PS and PP combine with the peptides in DI water and 3.5% NaCl solution regardless of surface oxidation, this method can be advantageous for detecting both unoxidized and oxidized microplastics in the ocean. Based on this method, it is possible to determine the extent of changes in the environmental pollution levels. However, in this study, during the process of obtaining oxidized microplastics, the plastic bead surfaces were oxidized and then pulverised. As a result, not all microplastic surfaces were oxidized to the same extent. In addition, since the selectivity of only one of the peptides has been validated in this study, more peptide affinity and selectivity studies must be conducted in the future. Furthermore, the microplastic samples used in this study were limited to one size range. In future studies, we plan to investigate the effect of microplastic size on the peptide-binding affinity. In addition, other plastic-binding peptides will be evaluated, and their plastic-binding efficiencies will be analysed.

## Author contributions

H. W., M. T., M. O., and J. C. designed the experiments. H. W., Y. K., and Y. C. performed data analysis. J. C. supervised the study. H. W., Y. K., and Y. C. prepared the graphics. H. W., M. T., M. O., J. S. K, and J. C. wrote the manuscript.

## Conflicts of interest

There are no conflicts to declare.

## Acknowledgements

This research was supported by the Chung-Ang University Research Scholarship Grants in 2020 (H. W.). This work was also supported by the National Research Foundation of Korea (NRF) grant funded by the Korea government (MSIT) (No. 2020R1A5A1018052).

## References

- 1 M. Sharifinia, Z. A. Bahmanbeigloo, M. Keshavarzifard, M. H. Khanjani and B. P. Lyons, Microplastic pollution as a grand challenge in marine research: A closer look at their adverse impacts on the immune and reproductive systems, *Ecotoxicol. Environ. Saf.*, 2020, **204**, 111109.
- 2 A. A. Horton and D. K. A. Barnes, Microplastic pollution in a rapidly changing world: Implications for remote and vulnerable marine ecosystems, *Sci. Total Environ.*, 2020, **738**, 140349.
- 3 E. Guzzetti, A. Sureda, S. Tejada and C. Faggio, Microplastic in marine organism: Environmental and toxicological effects, *Environ. Toxicol. Pharmacol.*, 2018, **64**, 164–171.
- 4 S. Sharma and S. Chatterjee, Microplastic pollution, a threat to marine ecosystem and human health: a short review, *Environ. Sci. Pollut. Res. Int.*, 2017, **24**(27), 21530–21547.
- 5 A. E. Schwarz, T. N. Ligthart, E. Boukris and T. van Harmelen, Sources, transport, and accumulation of different types of plastic litter in aquatic environments: A review study, *Mar. Pollut. Bull.*, 2019, **143**, 92–100.
- 6 T. Huffer, A. Praetorius, S. Wagner, F. von der Kammer and T. Hofmann, Microplastic Exposure Assessment in Aquatic Environments: Learning from Similarities and Differences to Engineered Nanoparticles, *Environ. Sci. Technol.*, 2017, **51**(5), 2499–2507.
- 7 R. Dris, J. Gasperi, C. Mirande, C. Mandin, M. Guerrouache, V. Langlois and B. Tassin, A first overview of textile fibers, including microplastics, in indoor and outdoor environments, *Environ. Pollut.*, 2017, **221**, 453–458.
- 8 S. Abbasi, N. Soltani, B. Keshavarzi, F. Moore, A. Turner and M. Hassanaghaei, Microplastics in different tissues of fish and prawn from the Musa Estuary, Persian Gulf, *Chemosphere*, 2018, **205**, 80–87.
- 9 T. Wang, X. Zou, B. Li, Y. Yao, Z. Zang, Y. Li, W. Yu and W. Wang, Preliminary study of the source apportionment and diversity of microplastics: Taking floating microplastics in the South China Sea as an example, *Environ. Pollut.*, 2019, **245**, 965–974.
- 10 F. Wang, C. S. Wong, D. Chen, X. Lu, F. Wang and E. Y. Zeng, Interaction of toxic chemicals with microplastics: A critical review, *Water Res.*, 2018, **139**, 208–219.
- 11 H. S. Auta, C. U. Emenike and S. H. Fauziah, Distribution and importance of microplastics in the marine environment: A review of the sources, fate, effects, and potential solutions, *Environ. Int.*, 2017, **102**, 165–176.
- 12 PlasticsEurope, *Plastics—The Facts 2020*. PlasticsEurope 2020, vol. 1, pp. 1–64.
- 13 I. Acosta-Coley and J. Olivero-Verbel, Microplastic resin pellets on an urban tropical beach in Colombia, *Environ. Monit. Assess.*, 2015, **187**(7), 435.
- 14 S. Veerasingam, M. Saha, V. Suneel, P. Vethamony, A. C. Rodrigues, S. Bhattacharyya and B. G. Naik, Characteristics, seasonal distribution and surface degradation features of microplastic pellets along the Goa coast, India, *Chemosphere*, 2016, **159**, 496–505.
- 15 X. Y. Qu, L. Su, H. X. Li, M. Z. Liang and H. H. Shi, Assessing the relationship between the abundance and properties of microplastics in water and in mussels, *Sci. Total Environ.*, 2018, **621**, 679–686.
- 16 C. Zhang, X. Chen, J. Wang and L. Tan, Toxic effects of microplastic on marine microalgae *Skeletonema costatum*: Interactions between microplastic and algae, *Environ. Pollut.*, 2017, **220**(Pt B), 1282–1288.
- 17 Y. K. Muller, T. Wernicke, M. Pittroff, C. S. Witzig, F. R. Storck, J. Klinger and N. Zumbulte, Microplastic analysis—are we measuring the same? Results on the first global comparative study for microplastic analysis in a water sample, *Anal. Bioanal. Chem.*, 2020, **412**(3), 555–560.
- 18 M. Claessens, L. Van Cauwenberghe, M. B. Vandegehuchte and C. R. Janssen, New techniques for the detection of



- microplastics in sediments and field collected organisms, *Mar. Pollut. Bull.*, 2013, **70**(1–2), 227–233.
- 19 G. Liebezeit and F. Dubaish, Microplastics in beaches of the East Frisian islands Spiekeroog and Kachelotplate, *Bull. Environ. Contam. Toxicol.*, 2012, **89**(1), 213–217.
  - 20 M. Lang, X. Yu, J. Liu, T. Xia, T. Wang, H. Jia and X. Guo, Fenton aging significantly affects the heavy metal adsorption capacity of polystyrene microplastics, *Sci. Total Environ.*, 2020, **722**, 137762.
  - 21 A. S. Tagg, J. P. Harrison, Y. Ju-Nam, M. Sapp, E. L. Bradley, C. J. Sinclair and J. J. Ojeda, Fenton's reagent for the rapid and efficient isolation of microplastics from wastewater, *Chem. Commun.*, 2016, **53**(2), 372–375.
  - 22 R. Lenz, K. Enders, C. A. Stedmon, D. M. A. Mackenzie and T. G. Nielsen, A critical assessment of visual identification of marine microplastic using Raman spectroscopy for analysis improvement, *Mar. Pollut. Bull.*, 2015, **100**(1), 82–91.
  - 23 S. Veerasingam, M. Ranjani, R. Venkatachalapathy, A. Bagaev, V. Mukhanov, D. Litvinyuk, M. Mugilarasan, K. Gurumoorthi, L. Gunganathan, V. M. Aboobacker and P. Vethamony, Contributions of Fourier transform infrared spectroscopy in microplastic pollution research: A review, *Crit. Rev. Environ. Sci. Technol.*, 2020, 1–63.
  - 24 A. B. Labbe, C. R. Bagshaw and L. Uttal, Inexpensive Adaptations of Basic Microscopes for the Identification of Microplastic Contamination Using Polarization and Nile Red Fluorescence Detection, *J. Chem. Educ.*, 2020, **97**(11), 4026–4032.
  - 25 J. C. Prata, V. Reis, J. T. V. Matos, J. P. da Costa, A. C. Duarte and T. Rocha-Santos, A new approach for routine quantification of microplastics using Nile Red and automated software (MP-VAT), *Sci. Total Environ.*, 2019, **690**, 1277–1283.
  - 26 T. Stanton, M. Johnson, P. Nathanail, R. L. Gomes, T. Needham and A. Burson, Exploring the Efficacy of Nile Red in Microplastic Quantification: A Costaining Approach, *Environ. Sci. Technol. Lett.*, 2019, **6**(10), 606–611.
  - 27 M. Farré, Remote and *in situ* devices for the assessment of marine contaminants of emerging concern and plastic debris detection, *Curr. Opin. Environ. Sci. Health*, 2020, **18**, 79–94.
  - 28 C. Contado, D. Mehn, D. Gilliland and L. Calzolari, Characterization methods for studying protein adsorption on nano-polystyrene beads, *J. Chromatogr. A*, 2019, **1606**, 460383.
  - 29 N. Trier, P. Hansen and G. Houen, Peptides, Antibodies, Peptide Antibodies and More, *Int. J. Mol. Sci.*, 2019, **20**(24), 6289.
  - 30 L. Apitius, K. Rubsam, C. Jakesch, F. Jakob and U. Schwaneberg, Ultrahigh-throughput screening system for directed polymer binding peptide evolution, *Biotechnol. Bioeng.*, 2019, **116**(8), 1856–1867.
  - 31 E. T. Boder and K. D. Wittrup, Yeast surface display for screening combinatorial polypeptide libraries, *Nat. Biotechnol.*, 1997, **15**(6), 553–557.
  - 32 Y. Kumada, Y. Tokunaga, H. Imanaka, K. Imamura, T. Sakiyama, S. Katoh and K. Nakanishi, Screening and characterization of affinity peptide tags specific to polystyrene supports for the orientated immobilization of proteins, *Biotechnol. Prog.*, 2006, **22**(2), 401–405.
  - 33 B. Bakhshinejad and M. Sadeghizadeh, A polystyrene binding target-unrelated peptide isolated in the screening of phage display library, *Anal. Biochem.*, 2016, **512**, 120–128.
  - 34 C. C. Dupont-Gillain, Y. Adriaensen, S. Derclaye and P. G. Rouxhet, Plasma-Oxidized Polystyrene: Wetting Properties and Surface Reconstruction, *Langmuir*, 2000, **16**(21), 8194–8200.
  - 35 E. Occhiello, M. Morra, P. Cinquina and F. Garbassi, Hydrophobic recovery of oxygen-plasma-treated polystyrene, *Polymer*, 1992, **33**(14), 3007–3015.
  - 36 N. Li, J. Kang, L. Jiang, B. He, H. Lin and J. Huang, PSBinder: A Web Service for Predicting Polystyrene Surface-Binding Peptides, *Biomed. Res. Int.*, 2017, **2017**, 5761517.
  - 37 M. Vodnik, B. Štrukelj and M. Lunder, HWGMWSY, an unanticipated polystyrene binding peptide from random phage display libraries, *Anal. Biochem.*, 2012, **424**(2), 83–86.
  - 38 Q. W. Cheng, S. R. Fahnestock, H. He, K. N. Kostichka, and H. Wang, Peptide linkers for effective multivalent peptide binding, *United States Patent*, Patent No.: US 8697654 B2, 2016.
  - 39 M. Masrurroh, D. Santjojo, A. Abdurrouf, M. A. A. Mahbub, M. Padaga and S. Sakti, Effect of Electron Density and Temperature in Oxygen Plasma Treatment of Polystyrene Surface, *IOP Conf. Ser.: Mater. Sci. Eng.*, 2019, **515**, 012061.
  - 40 S. Aslanzadeh and M. Haghighat Kish, Photo-oxidation of polypropylene fibers exposed to short wavelength UV radiations, *Fibers Polym.*, 2010, **11**(5), 710–718.
  - 41 B. Maillhot and J. L. Gardette, Polystyrene photooxidation. 1. Identification of the IR-absorbing photoproducts formed at short and long wavelengths, *Macromolecules*, 1992, **25**(16), 4119–4126.
  - 42 H. reisi nafchi, M. Abdouss, S. Kazemi, R. Mohebbi Gargari and M. Mazhar, Effects of nano-clay particles and oxidized polypropylene polymers on improvement of the thermal properties of wood plastic composite, *Maderas: Cienc. Tecnol.*, 2015, **17**, 45–54.
  - 43 A. Dyachenko, J. Mitchell and N. Arsem, Extraction and identification of microplastic particles from secondary wastewater treatment plant (WWTP) effluent, *Anal. Methods*, 2017, **9**(9), 1412–1418.
  - 44 Y. Kumada, D. Kuroki, H. Yasui, T. Ohse and M. Kishimoto, Characterization of polystyrene-binding peptides (PS-tags) for site-specific immobilization of proteins, *J. Biosci. Bioeng.*, 2010, **109**(6), 583–587.
  - 45 J. M. Kogot, D. A. Sarkes, I. Val-Addo, P. M. Pellegrino and D. N. Stratis-Cullum, Increased affinity and solubility of peptides used for direct peptide ELISA on polystyrene surfaces through fusion with a polystyrene-binding peptide tag, *BioTechniques*, 2012, **52**(2), 95–102.
  - 46 J. B. Tang, X. F. Sun, H. M. Yang, B. G. Zhang, Z. J. Li, Z. J. Lin and Z. Q. Gao, Well-oriented ZZ-PS-tag with high Fc-binding onto polystyrene surface for controlled immobilization of capture antibodies, *Anal. Chim. Acta*, 2013, **776**, 74–78.





- 47 Y. Kumada, Y. Shiritani, K. Hamasaki, T. Ohse and M. Kishimoto, High biological activity of a recombinant protein immobilized onto polystyrene, *Biotechnol. J.*, 2009, **4**(8), 1178–1189.
- 48 T. Sakiyama, S. Ueno, K. Imamura and K. Nakanishi, Use of a novel affinity tag selected with a bacterial random peptide library for improving activity retention of glutathione S-transferase adsorbed on a polystyrene surface, *J. Mol. Catal. B: Enzym.*, 2004, **28**(4), 207–214.
- 49 H. Imanaka, D. Yamadzuki, K. Yanagita, N. Ishida, K. Nakanishi and K. Imamura, The use of a proteinaceous “cushion” with a polystyrene-binding peptide tag to control the orientation and function of a target peptide adsorbed to a hydrophilic polystyrene surface, *Biotechnol. Prog.*, 2016, **32**(2), 527–534.
- 50 Y. Kumada, K. Hamasaki, Y. Shiritani, A. Nakagawa, D. Kuroki, T. Ohse, D. H. Choi, Y. Katakura and M. Kishimoto, Direct immobilization of functional single-chain variable fragment antibodies (scFvs) onto a polystyrene plate by genetic fusion of a polystyrene-binding peptide (PS-tag), *Anal. Bioanal. Chem.*, 2009, **395**(3), 759–765.
- 51 K. RübSam, M. D. Davari, F. Jakob and U. Schwaneberg, KnowVolution of the Polymer-Binding Peptide LCI for Improved Polypropylene Binding, *Polymers*, 2018, **10**(4), 423.
- 52 K. RübSam, B. Stomps, A. Böker, F. Jakob and U. Schwaneberg, Anchor peptides: A green and versatile method for polypropylene functionalization, *Polymer*, 2017, **116**, 124–132.
- 53 Y. Kumada, S. Katoh, H. Imanaka, K. Imamura and K. Nakanishi, Development of a one-step ELISA method using an affinity peptide tag specific to a hydrophilic polystyrene surface, *J. Biotechnol.*, 2007, **127**(2), 288–299.
- 54 Y. R. Corrales-Ureña, Z. Souza-Schiaber, P. N. Lisboa-Filho, F. Marquet, P.-L. Michael Noeske, L. Gätjen and K. Rischka, Functionalization of hydrophobic surfaces with antimicrobial peptides immobilized on a bio-interfacial layer, *RSC Adv.*, 2020, **10**(1), 376–386.
- 55 O. Mermut, D. C. Phillips, R. L. York, K. R. McCrea, R. S. Ward and G. A. Somorjai, *In situ* adsorption studies of a 14-amino acid leucine-lysine peptide onto hydrophobic polystyrene and hydrophilic silica surfaces using quartz crystal microbalance, atomic force microscopy, and sum frequency generation vibrational spectroscopy, *J. Am. Chem. Soc.*, 2006, **128**(11), 3598–3607.
- 56 H.-N. S. In-San Kim *Polypeptide binding polystyrene specifically and use thereof*. 2013.
- 57 T. Lin, W. Guo, R. Guo and Z. Chen, Probing Biological Molecule Orientation and Polymer Surface Structure at the Polymer/Solution Interface *In Situ*, *Langmuir*, 2020, **36**(26), 7681–7690.
- 58 M. M. Flocco and S. L. Mowbray, Planar stacking interactions of arginine and aromatic side-chains in proteins, *J. Mol. Biol.*, 1994, **235**(2), 709–717.
- 59 G. Duan, V. H. Smith and D. F. Weaver, Characterization of Aromatic–Amide (Side-Chain) Interactions in Proteins through Systematic *ab Initio* Calculations and Data Mining Analyses, *J. Phys. Chem. A*, 2000, **104**(19), 4521–4532.
- 60 Z. Feng, T. Zhang, Y. Li, X. He, R. Wang, J. Xu and G. Gao, The accumulation of microplastics in fish from an important fish farm and mariculture area, Haizhou Bay, China, *Sci. Total Environ.*, 2019, **696**, 133948.
- 61 J. Wang, X. Liu, G. Liu, Z. Zhang, H. Wu, B. Cui, J. Bai and W. Zhang, Size effect of polystyrene microplastics on sorption of phenanthrene and nitrobenzene, *Ecotoxicol. Environ. Saf.*, 2019, **173**, 331–338.

